

Experimental Study of Natural Convection in a Partially Porous Enclosure

S. B. Sathe* and T. W. Tong†
Arizona State University, Tempe, Arizona
 and
 M. A. Faruque‡
Intel Corporation, Santa Clara, California

This paper presents the experimental results for steady-state natural convection heat transfer in a rectangular enclosure. The enclosure was divided vertically with an impermeable partition into a fluid-saturated porous region and a fluid-filled region. The horizontal boundaries of the enclosure were adiabatic and the vertical boundaries were isothermal. Experimental runs were carried out for different porous materials, Rayleigh numbers, and thicknesses of the porous region. The results verified an earlier prediction that the heat transfer could be minimized by partially filling the enclosure with a porous material rather than filling it entirely. A correlation has been developed expressing the Nusselt number in terms of the relevant governing parameters.

Nomenclature

a_0, a_1, a_2	= constants in Eq. (4)
A	= aspect ratio of the enclosure, L/d
A_0	= area of heat transfer in the enclosure test apparatus
A_1	= area of heat transfer in the thermal conductivity test enclosure
b_0, b_1, b_2	= constants in Eq. (4)
c	= specific heat of fluid at constant pressure
C	= variable in Eq. (4)
d	= width of the enclosure
d_0	= average pore diameter of the porous material
Da	= Darcy number, κ/d^2
g	= acceleration due to gravity
k	= thermal conductivity
L	= height of the enclosure
L_0	= distance between pressure tapings in the permeability test duct
Nu	= Nusselt number
p	= pressure
Δp	= pressure difference
Pr	= Prandtl number, $\mu/\rho\alpha_f$
Q	= heat input in the thermal conductivity test apparatus
Q_0	= heat input in the enclosure test
R_c	= ratio of thermal conductivities, k_f/k_{eff}
Ra	= Rayleigh number, $\rho g \beta (T_h - T_c) d^3 / \mu \alpha_f$
Ra_0	= modified Rayleigh number, $\rho g \beta (T_h - T_c) \kappa d / \mu \alpha_p$
Re	= Reynolds number based on pore diameter, $\rho U d_0 / \mu$
s	= width of enclosure occupied by the porous material
S	= porous fraction, s/d
T	= temperature

ΔT	= difference between the hot and the cold plate temperatures, $T_h - T_c$
U	= average velocity in the permeability test apparatus
Δx	= spacing between hot and cold wall in the thermal conductivity test apparatus
α	= thermal diffusivity, $k/\rho c$
β	= coefficient of volumetric expansion
κ	= permeability
μ	= dynamic viscosity
ρ	= density of fluid

Subscripts

av	= average
c	= cold
eff	= effective
f	= fluid
m	= mean
p	= porous

Introduction

IN a numerical study, Tong and Subramanian¹ found that heat transfer could go through a minimum when a rectangular enclosure, originally occupied by a fluid, was gradually filled with a porous medium saturated with the same fluid. This finding suggests that an enclosure need not be entirely filled with a porous material to achieve the maximum insulating effect. Hence, insulation usages can potentially be optimized, resulting in lower capital and operating costs of insulation systems.

The aim of the present study is twofold: 1) to verify experimentally the finding of Tong and Subramanian,¹ and 2) to generate experimental results for heat transfer in enclosures partially filled with a porous medium. The enclosure considered by Tong and Subramanian¹ was assumed to have isothermal vertical walls and adiabatic horizontal walls. A schematic diagram is shown in Fig. 1. The porous and the fluid regions were separated by an impermeable partition with negligible temperature difference across it. An enclosure with an aspect ratio of 10 was fabricated to simulate the situation shown in Fig. 1.

In insulation applications, the solid matrix of the porous medium is a material with low thermal conductivity. For ex-

Received May 22, 1986; revision received Sept. 1, 1986. Copyright © American Institute of Aeronautics and Astronautics, Inc., 1987. All rights reserved.

*Research Assistant, Department of Mechanical and Aerospace Engineering.

†Associate Professor, Department of Mechanical and Aerospace Engineering. Member AIAA.

‡Product Engineer.

ample, glass fibers are used extensively in building insulations. However, fiberglass insulations are quite compressible, and their physical characteristics, such as thickness and porosity, are difficult to define accurately. Consequently, Nickel Foametal (a porous material made of commercial nickel) and foam plastic (polyurethane foam) slabs of definite size and shape were used as the test material in this study. For most porous insulations, the ratio of the fluid thermal conductivity to the effective thermal conductivity of the porous material saturated with the same fluid (R_c) is either less than 1 or approximately equal to 1. To simulate such conditions, distilled water was used with the Nickel Foametal and foam plastic to achieve R_c less than 1 and approximately 1, respectively.

Experimental Program

The dimensionless governing equations for heat transfer through partially porous enclosures, as considered in Ref. 1, show that the governing parameters for the heat transfer are A , Pr , Ra , Da , R_c , Ra_0 , and S , where A is the aspect ratio of the enclosure, Pr the Prandtl number of the fluid, Ra the Rayleigh number, Da the Darcy number, R_c the ratio of the thermal conductivity of the fluid to the effective thermal conductivity of the porous medium saturated with the same fluid, Ra_0 the modified Rayleigh number, and S the dimensionless thickness of the porous region. The definitions of the variables involved in describing these parameters can be found in the Nomenclature. Since $Ra_0 = RaDaR_c$, only three of these four parameters are independent.

The determination of the governing parameters in the experiments required the evaluation of the following thermophysical properties: μ , c_f , k_f , ρ , κ , k_{eff} , and β . The thermal diffusivities α_f and α_p were calculated from the relations $\alpha_f = k_f / \rho c_f$ and $\alpha_p = k_{eff} / \rho c_f$. Since κ and k_{eff} were the only two properties that were not available in the literature, experiments were conducted to measure κ and k_{eff} for both Nickel Foametal and foam plastic saturated with distilled water. The rest of the thermophysical properties were evaluated at the arithmetic mean temperature of the hot and cold walls from values reported in the literature.

Permeability Measurement

The Darcy's equation for fluid flow through a porous medium is

$$U = \kappa \Delta p / (\mu L_0) \quad (1)$$

where U is the average velocity of the fluid, κ the permeability of the porous medium saturated with the fluid, Δp the pressure drop over a length L of the porous material, and μ the dynamic viscosity of the fluid. This equation is valid only when the Reynolds number (Re) based on the pore diameter of the porous material is less than 4.0.² In the present work, the upper limit of Re is 2.94 for Nickel Foametal³ and 3.33 for foam plastic.⁴

The apparatus for measuring the permeability of Nickel Foametal is shown schematically in Fig. 2. The test region was a rectangular Plexiglas duct with a flow cross section of 0.1270 m \times 0.0254 m. It was completely filled with 12 Nickel Foametal slabs, each measuring 0.2032 m \times 0.1270 m \times 0.0064 m. The total length of the porous column was 0.6096 m. The duct was mounted vertically onto a wall. For measuring the pressure drop, two tappings were drilled 0.5080 m apart on one side of the duct. Distilled water was circulated through the system as shown in Fig. 2. A constant water level was maintained in the overhead reservoir, so that the flow through the duct remained constant for a particular valve setting. A Validyne CD-12 transducer-meter system was used to measure the pressure drop. A thermometer was installed in the overhead tank to measure the water temperature.

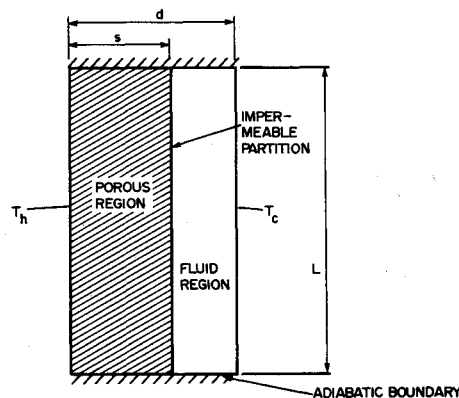


Fig. 1 Partially porous enclosure.

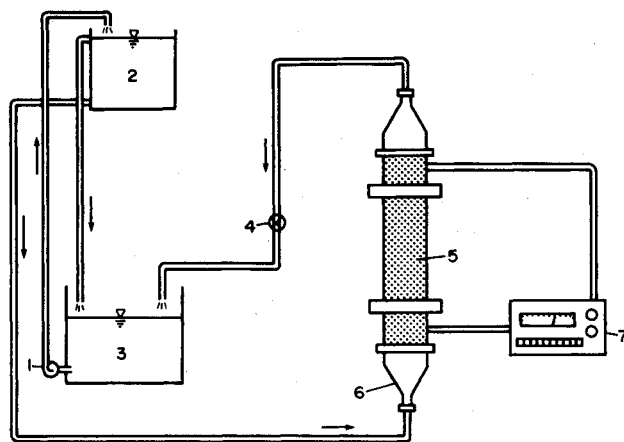


Fig. 2 Schematic diagram of the permeability test apparatus: 1) pump, 2) overhead reservoir, 3) sump tank, 4) valve, 5) porous material, 6) test duct, and 7) pressure-transducer.

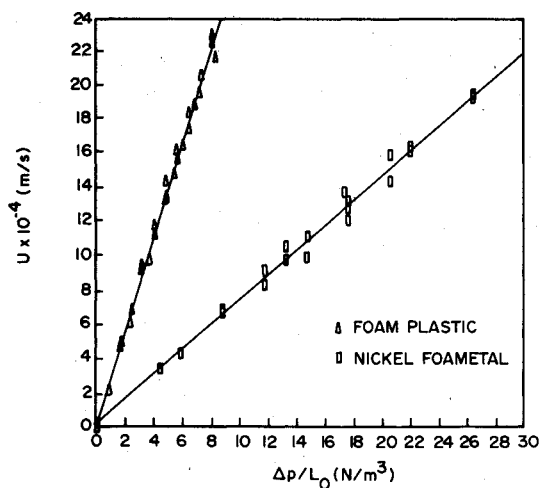


Fig. 3 Average velocity U (m/s) vs $\Delta p/L_0$ (N/m^3).

The flow rate through the duct was maintained at a particular value until steady state was attained (i.e., when the flow rate and the pressure drop remained constant). The flow rate was measured by the catch and weigh method. The pressure drop across the tappings and the water temperature were measured. The procedure was repeated for different flow rates obtained by adjusting the valve downstream of the duct.

Figure 3 shows the average velocity U through the test duct plotted against the pressure drop per unit length of the duct ($\Delta p/L_0$). A least-squares error approximation (software

package ENERGRAPHICS) was used to find a straight line passing through the data. The variance of the data points about this line shown in Fig. 3 is 2.43×10^{-3} . It can be seen from Eq. (1) that the slope of this line is κ/μ . The viscosity was evaluated at the measured water temperature (24°C), and the permeability was calculated to be $\kappa = 6.76 \times 10^{-8} \text{ m}^2$. The uncertainty in the value of κ was estimated to be $\pm 6.21\%$.³

The apparatus shown in Fig. 2 was used to measure the permeability of the foam plastic. The duct length was extended so that the porous column in this case was 1.219 m long and had pressure tapings 1.127 m apart. The permeability of the foam plastic was calculated in much the same manner as the permeability of Nickel Foametal. The average velocity U through the test duct against the pressure drop per unit length of the duct ($\Delta p/L_0$) is plotted in Fig. 3. Using the procedure mentioned in the preceding paragraph, a straight line was fitted through the data. The variance for this case was 2.16×10^{-2} . The permeability of the foam plastic was calculated as $\kappa = 2.369 \times 10^{-7} \text{ m}^2$, with an uncertainty of $\pm 2.98\%$.⁴

Effective Thermal Conductivity Measurement

An apparatus was built to simulate steady-state conductive heat transfer across a 0.0064-m-thick slab of porous material (Nickel Foametal or foam plastic) measuring 0.1270 m \times 0.2032 m, saturated with distilled water.

From Fourier's law of heat conduction, we have

$$Q = k_{\text{eff}} A_1 \Delta T / \Delta x \quad (2)$$

where Q is the thermal energy per unit time transferred across the slab, A_1 the area perpendicular to the direction of the heat flow (0.1270 m \times 0.2032 m), ΔT the temperature difference between the two faces of the slab, and Δx the slab thickness (0.0064 m). Hence, k_{eff} can be determined if the other variables in Eq. (2) are measured experimentally.

The apparatus used is shown schematically in Fig. 4. It was an enclosure with isothermal horizontal walls (hot and cold plates) and vertical adiabatic walls (Plexiglas plates, insulated with Styrofoam). The vertical walls were bolted to the hot and cold plates to form the enclosure. The cavity of the enclosure was completely occupied by the porous material saturated with distilled water. The enclosure was oriented with the hot plate on top in order to provide a stabilizing temperature gradient to prevent convection from taking place. The hot and cold plates were 0.0095-m-thick copper plates measuring 0.1270 m \times 0.2032 m each. An electrical heater (the main heater), made of Nichrome strips sandwiched between two thin mica sheets, was placed on top of the hot plate to supply heat to the hot plate. A 0.0032-m Teflon sheet was placed on top of the main heater. A 0.0095-m-thick copper guard plate, 0.1270 m \times 0.2032 m, was placed on top of this Teflon sheet. Another heater (the guard heater) was placed on top of the guard plate to supply heat to the guard plate. The guard plate and the guard heater were necessary to prevent heat loss from the main heater in the direction opposite to the hot plate. This was achieved by maintaining the guard plate and the hot plate at the same temperature. The apparatus was not guarded in the horizontal direction because of the edge heat loss from the hot plate was estimated to be less than 1.5% of the heat transfer across the specimen, assuming the edges were not insulated.³ Since the edges were isolated from the surroundings by the 0.0064-m-thick Plexiglas vertical walls, and the entire apparatus was insulated with 0.0254-m-thick Styrofoam, the actual edge heat loss was much smaller than the estimated value.

Copper-constantan thermocouples (gage 30) were used for temperature measurements. All the thermocouples were made from the same spool of thermocouple wire. A sample thermocouple was calibrated against a calibrated chromel-

constantan thermocouple obtained from the Metals and Ceramics Division at the Oak Ridge National Laboratory.³

Six thermocouples and a temperature sensor (RFL model 27687-5) were installed in the grooves made on the upward-facing surface of the hot plate. Four thermocouples and a sensor (RFL model 46911) were installed on the upward-facing surface of the guard plate. Similarly, six thermocouples were installed on the downward-facing surface of the cold plate. The thermocouples on each plate were distributed over the entire plate area. The locations of the thermocouples and the temperature sensors on the plates can be found in Ref. 3.

The cold plate had copper cooling tubes soldered on its downward-facing surface. The cold plate was cooled by circulating cooling water through these tubes from a constant temperature bath (NESLAB RTE4), which had a heater and a refrigeration unit, so that the temperature of the cooling water could be adjusted as desired.

The hot plate temperature was controlled by a RFL 72-A proportional temperature controller, which could be set for a desired temperature. The temperature controller automatically regulated the electrical power supply to the main heater, depending on the signal it received from the temperature sensor, by proportionally spacing the power pulses in time. Similarly, a RFL 71-A temperature controller was used to control the guard plate temperature. A power-pulse meter was used to count the power pulses delivered to the main heater in a certain time period. When the rms value of the voltage drop across the main heater and the resistance of the main heater are known, the actual average power

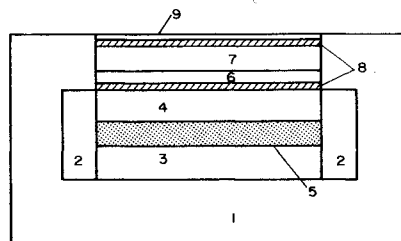


Fig. 4 Schematic diagram of the apparatus for the thermal conductivity test: 1) Styrofoam, 2) Plexiglas, 3) cold plate, 4) hot plate, 5) porous material, 6) Teflon sheet, 7) guard plate, 8) heaters, and 9) thin layer of packing sponge.

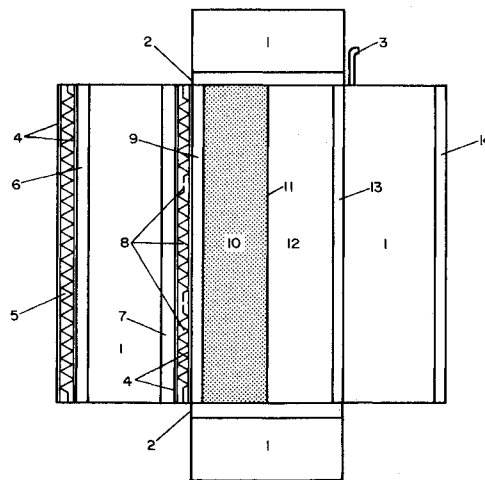


Fig. 5 Schematic diagram of the enclosure apparatus: 1) Styrofoam, 2) Plexiglas, 3) cooling tube, 4) mica sheet, 5) guard heater, 6) guard plate, 7) cardboard, 8) main heaters, 9) hot plate, 10) porous material, 11) impermeable partition, 12) fluid, 13) cold plate, and 14) wooden plank.

delivered to the main heater can be determined. The average power corresponded to Q in Eq. (2).

Five runs were carried out with three different Nickel Foametal specimens. Twelve runs were also carried out with three different samples of foam plastic. For each measurement, the average temperature of the hot and cold wall (T_m) was kept close to the ambient temperature to minimize heat losses from the enclosure. The hot, cold, and guard plates were kept isothermal to within $\pm 0.05^\circ\text{C}$. The system was allowed to run for 5–6 h to achieve steady state. A logging multimeter (HP 3467A) was used to record the emf (in mV) from the thermocouples. The millivolt values were then converted to degrees Celsius using the calibrated data in Ref. 3. The power-pulse meter was run for 5–10 min, and the number of pulses over this time was recorded. Equation (2) was used to calculate k_{eff} . The average k_{eff} of Nickel Foametal from the eight measurements was $0.869 \text{ W/m}^\circ\text{C}$. An error analysis revealed an uncertainty of $\pm 10.35\%$ in the value of k_{eff} . The average k_{eff} of foam plastic from 12 runs was calculated as $0.599 \text{ W/m}^\circ\text{C}$, with an uncertainty of $\pm 5.17\%$. However, the actual variation in the measured k_{eff} was $\pm 1.5\%$ for Nickel Foametal and $\pm 1.7\%$ for foam plastic.

Enclosure Heat-Transfer Measurement

Experiments were conducted to simulate the situation in Fig. 1, and the heat-transfer rates across the enclosure were measured. The apparatus used is shown schematically in Fig. 5. It was constructed such that the inside dimensions were 0.2540 m high and 0.0254 m wide so that the aspect ratio of the enclosure was 10. The depth was 0.4064 m. The apparatus consisted of two vertical copper plates (the hot and the cold walls), each measuring $0.4064 \text{ m} \times 0.2540 \text{ m} \times 0.0095 \text{ m}$. The top and the bottom walls were made of 0.095-m-thick Plexiglas plates bolted to the hot and the cold walls. The vertical end walls were 0.0064-m-thick Plexiglas plates bolted to the hot and the cold wall to form an enclosure. A 0.0008-m-thick copper plate measuring $0.4064 \text{ m} \times 0.2540 \text{ m}$ was used as the impermeable partition to separate the porous and fluid regions. For the limiting cases of $S=0$ and 1, the copper plate was removed from the enclosure. The guard plate was a copper plate, $0.4064 \text{ m} \times 0.2540 \text{ m} \times 0.0095 \text{ m}$, placed across a 0.0032-m-thick cardboard and a 0.0508-m-thick Styrofoam slab behind the hot plate (on the outer side of the enclosure). The cold plate was covered by a 0.0508-m-thick Styrofoam slab and a 0.0064-m-thick wooden plank. The whole apparatus was well insulated from the surroundings with insulating foam.

The hot and guard plates were heated by the main heater and the guard heater, respectively. The heaters were 0.0127-

m-wide Nichrome strips sandwiched between thin mica sheets. The main heater had three separate heater segments controlled independently by three sets of sensor-controller arrangements. Separate heater segments were needed to maintain the hot plate at a uniform temperature.

Eleven thermocouples were attached to the hot plate. Similarly, five thermocouples were attached to the guard plate, and seven thermocouples were attached to the cold plate. The locations of the thermocouples on the hot and guard plates can be found in Ref. 3.

One temperature sensor (RFL model 46911) was embedded in the guard plate and connected to a RFL 71-A temperature controller. Similarly, three temperature sensors (RFL model 27686-5) were installed on the hot plate, each positioned in the area heated by the respective heater segment. The temperature sensors were connected to three separate proportional temperature controllers (RFL model 72-A). Electrical power was supplied to the respective heater segments through the temperature controllers. The power supply to the heater segments of the main heater was measured by the power-pulse meter.

The cold plate was cooled by circulating cold water from a constant-temperature bath (NESLAB RTE4) through two 0.0064-m-diam copper tubes soldered on the surface of the cold plate surface facing away from the cavity. The cooling water was circulated through the cooling tubes in a counterflow fashion, and the layout of the cooling tubes can be found in Ref. 3.

Experiments were run with $A=10$, for $S=0, 0.25, 0.50, 0.75$, and 1.00 for Nickel Foametal. Whenever S was changed, it was necessary to disassemble the enclosure, reassemble it, and place the Nickel Foametal of an appropriate thickness in the enclosure to give the desired S . Similar experiments were carried out with foam plastic as the porous material.

For each combination of the porous material and S , several test runs were made at different hot and cold plate temperatures, while keeping T_m close to the ambient temperature. The hot, cold, and guard plates were kept isothermal within $\pm 0.05^\circ\text{C}$. The system was allowed to reach steady state before any data were recorded. It took approximately 8–10 h to reach steady state. A logging multimeter (HP 3467A) was used to record the mV readings of the thermocouples. The power input to each heater segment of the main heater was recorded using the power-pulse meter as described earlier in the procedure for the thermal conductivity test. The flow rate and the inlet and outlet temperatures of the cooling water were recorded for each of the two cooling circuits. This information was collected to check for the energy balance. It was done to

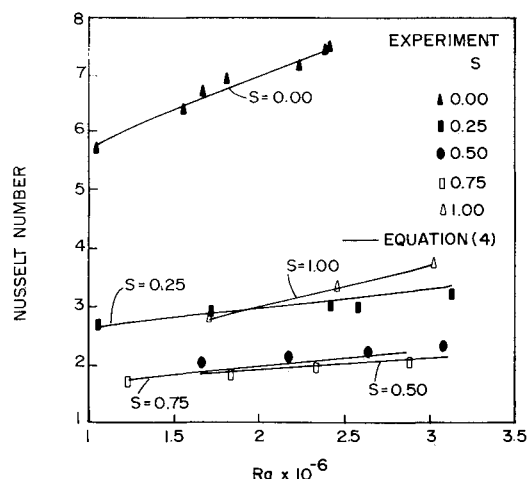


Fig. 6 Nusselt number for Nickel Foametal ($Da = 1.048 \times 10^{-4}$).

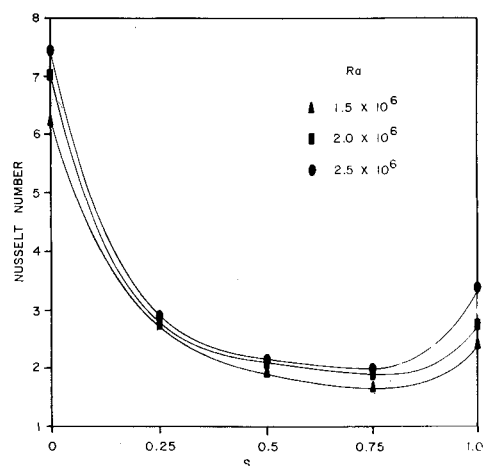


Fig. 7 Interpolated Nusselt number for Nickel Foametal ($Da = 1.048 \times 10^{-4}$).

ensure that there was no significant heat loss or gain through the top, bottom, and end walls of the enclosure. This heat loss or gain was found to be within 4.5% of the heat supplied by the hot plate. The edge heat loss from the hot plate was estimated to be less than 2% of the heat transfer across the enclosure.³

The Nusselt number (Nu) was defined as the ratio of the total heat transfer to the heat transfer by conduction when the entire enclosure was filled with fluid alone. It was defined in such a manner as to provide a common basis for comparing heat-transfer rates for different porous materials and S .

Hence,

$$Nu = Q_0 d / k_f A_0 \Delta T \quad (3)$$

where Q_0 is the total heat energy per unit time supplied by the main heater, d the enclosure width, A_0 the area of heat transfer ($0.2540 \text{ m} \times 0.4064 \text{ m}$), and ΔT the difference between the hot and the cold plate temperatures.

Results and Discussion

Shown in Tables 1 and 2 is a summary of the test conditions and results of all the experimental runs with Nickel Foametal and foam plastic, respectively, as the porous materials. Heat-transfer results are presented in terms of Nu as defined by Eq. (3). The uncertainties in the values of Nu ranged from $\pm 3.79\%$ to $\pm 8.35\%$. For the runs in which $S=0$, R_c and Ra_0 were meaningless and were not tabulated. The hot and cold wall temperatures are also included in Tables 1 and 2 in order to show the temperature ranges at which the measurements were made. All thermophysical properties of the test fluid were evaluated at the arithmetic mean of the wall temperatures.

The results in Table 1 are presented in a graphic form in Fig. 6. It can be seen that significant reduction in heat transfer was obtained when S was increased from 0 to 0.25. The amount of reduction in heat transfer became smaller as S was further increased from 0.25 to 0.50 and from 0.50 to 0.75. Heat transfer increased when S was changed from 0.75 to 1.00. It is clear that heat transfer went through a minimum as the enclosure was filled vertically with the Nickel Foametal. This trend can best be illustrated by plotting Nu as a function of S . At fixed values of Ra , Nusselt numbers for different S were interpolated from the results shown in Fig. 6, and they are represented by the symbols in Fig. 7. Each of the curves connecting the points with the same symbol was obtained by the method of least-squares error fit with a polynomial of fourth order. The curves show that Nu goes through a minimum as S is increased from 0 to 1. Figures 8 and 9 plot results similar to those in Figs. 6 and 7, but for foam plastic as the porous material. The existence of a minimum can be seen again in Fig. 9.

Since the Ra_0 values in this study were of the order of 10^2 and 10^3 , there was natural convective heat transfer in the fluid region as well as in the porous region. As S was increased from 0 to 1, there was a reduction in natural convective heat transfer in the fluid region. This occurred because the fluid region became narrower, and the intensity of convection in that region decreased. At the same time, however, the convective heat transfer in the porous region increased as a result of widening of the porous region. Also, as R_c for Nickel Foametal and foam plastic was less than 1 and approximately 1, respectively, the corresponding conductive heat transfer increased and remained the same when S was increased. The minimum in the case of Nickel Foametal occurred when the increase in convective heat transfer in the porous region combined with the increase in conductive heat transfer was offset by the decrease in convective heat transfer in the fluid region. In the case of foam plastic, the minimum occurred when the increase in convective heat transfer in the porous region was offset by the decrease in convective heat transfer in the fluid region.

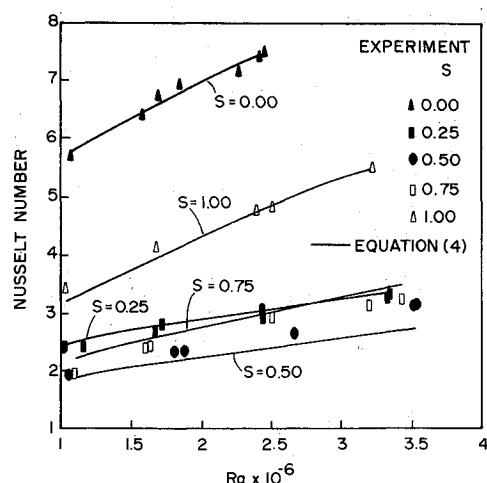


Fig. 8 Nusselt number for foam plastic ($Da = 3.672 \times 10^{-4}$).

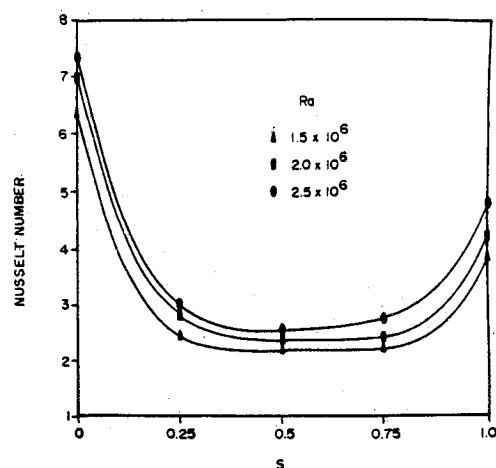


Fig. 9 Interpolated Nusselt number for foam plastic ($Da = 3.672 \times 10^{-4}$).

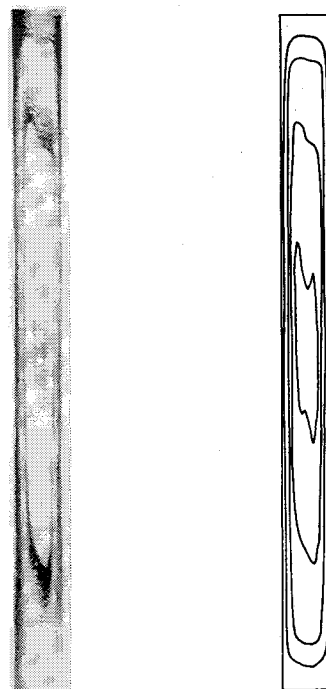


Fig. 10 Comparison of the photographed flow pattern and predicted streamlines in the fluid region for run 11, Table 1.

Table 1 Summary of experimental conditions and results. $A = 10$; $Da = 1.048 \times 10^{-4}$; porous material: Nickel Foametal

Run no.	S	Ra	R_c	Ra_0	Pr	$T_h, ^\circ C$	$T_c, ^\circ C$	Nu
1	0.00	1.06×10^6	—	—	6.35	25.45	21.80	5.66
2	0.00	1.57	—	—	6.11	27.61	22.68	6.33
3	0.00	1.68	—	—	6.32	26.68	20.97	6.66
4	0.00	1.83	—	—	6.19	27.60	21.64	6.87
5	0.00	2.25	—	—	6.05	28.96	22.02	7.09
6	0.00	2.40	—	—	6.08	29.02	21.51	7.36
7	0.00	2.43	—	—	6.30	28.05	19.86	7.43
8	0.25	1.07	0.702	78.7	6.18	26.42	22.96	2.67
9	0.25	1.73	0.702	127.4	6.15	27.68	22.16	2.89
10	0.25	2.44	0.702	179.6	6.19	28.55	20.62	2.98
11	0.25	2.60	0.702	191.3	6.15	28.64	20.13	2.97
12	0.25	3.15	0.702	231.8	6.19	29.70	19.46	3.21
13	0.50	1.68	0.700	123.2	6.34	26.61	20.86	2.00
14	0.50	2.19	0.702	161.1	6.19	28.18	21.05	2.12
15	0.50	2.65	0.702	195.0	6.15	29.13	20.67	2.20
16	0.50	3.10	0.703	228.5	6.05	30.24	20.69	2.30
17	0.75	1.25	0.698	91.7	6.46	25.17	20.67	1.67
18	0.75	1.84	0.699	135.1	6.46	26.26	19.66	1.81
19	0.75	2.34	0.699	171.7	6.40	27.41	19.19	1.92
20	0.75	2.90	0.697	211.9	6.58	27.59	16.69	2.00
21	1.00	1.72	0.700	126.2	6.30	26.83	21.01	2.75
22	1.00	2.47	0.702	181.7	6.11	29.03	21.24	3.30
23	1.00	3.04	0.703	224.0	6.07	30.07	20.64	3.70
24	1.00	4.77	0.702	351.2	6.18	32.46	17.03	4.74

Table 2 Summary of experimental conditions and results. $A = 10$; $Da = 3.672 \times 10^{-4}$; porous material: foam plastic

Run no.	S	Ra	R_c	Ra_0	Pr	$T_h, ^\circ C$	$T_c, ^\circ C$	Nu
1	0.00	1.06×10^6	—	—	6.35	25.45	21.80	5.66
2	0.00	1.57	—	—	6.11	27.61	22.68	6.33
3	0.00	1.68	—	—	6.32	26.68	20.97	6.66
4	0.00	1.83	—	—	6.19	27.60	21.64	6.87
5	0.00	2.25	—	—	6.05	28.96	22.02	7.09
6	0.00	2.40	—	—	6.08	29.02	21.51	7.36
7	0.00	2.43	—	—	6.30	28.05	19.86	7.43
8	0.25	1.02	1.018	381.3	6.15	26.50	23.24	2.35
9	0.25	1.16	1.018	433.6	6.18	26.53	22.79	2.38
10	0.25	1.67	1.018	624.3	6.23	27.17	21.68	2.65
11	0.25	1.71	1.018	639.2	6.15	27.65	22.21	2.76
12	0.25	2.43	1.018	908.4	6.18	28.62	20.76	3.03
13	0.25	2.43	1.018	908.4	6.18	28.64	20.79	2.90
14	0.25	3.33	1.018	1244.8	6.19	29.99	19.18	3.22
15	0.25	3.34	1.018	1248.5	6.18	30.10	19.32	3.31
16	0.50	1.06	1.018	396.2	6.16	26.47	23.07	1.91
17	0.50	1.81	1.018	676.6	6.16	27.74	21.95	2.29
18	0.50	1.88	1.020	704.1	6.11	28.19	22.31	2.32
19	0.50	2.66	1.018	994.3	6.21	28.84	20.15	2.60
20	0.50	3.51	1.017	1310.8	6.28	29.95	18.16	3.09
21	0.50	3.53	1.015	1315.7	6.34	29.77	17.69	3.12
22	0.75	1.10	1.015	410.0	6.23	26.32	22.72	1.91
23	0.75	1.61	1.018	601.8	6.16	27.44	22.30	2.38
24	0.75	1.63	1.015	607.5	6.23	27.07	21.72	2.43
25	0.75	2.50	1.020	936.4	6.10	29.13	21.30	2.89
26	0.75	3.19	1.018	1192.4	6.17	29.89	19.64	3.17
27	0.75	3.42	1.017	1277.2	6.26	29.89	18.52	3.24
28	1.00	1.02	1.018	381.2	6.18	26.33	23.05	3.35
29	1.00	1.67	1.018	624.3	6.16	27.47	22.12	4.07
30	1.00	2.38	1.018	889.7	6.22	28.34	20.55	4.69
31	1.00	2.49	1.018	930.8	6.11	29.04	21.18	4.74
32	1.00	3.21	1.018	1199.9	6.21	29.80	19.35	5.44

Table 3 Constants in Eq. (4)

Porous material	a_0	a_1	a_2	b_0	b_1	b_2
Nickel Foametal	0.01901	0.88119	0.39056	0.03579	0.35218	4.30859
Foam plastic	0.05339	0.62485	0.53845	0.02530	0.37617	5.04686

Table 4 Comparison of Nu for $S=0$

Ra	Pr	Nu	
		Present experiment	Experimental correlation from Seki et al. ⁵
1.06×10^6	6.35	5.66	5.54
1.57	6.11	6.33	6.10
1.68	6.32	6.66	6.22
1.83	6.19	6.87	6.34
2.25	6.05	7.09	6.67
2.40	6.08	7.36	6.78
2.43	6.30	7.43	6.82

Table 5 Comparison of Nu for $S=0.25, 0.50^a$

Porous material ^b	S	Ra	R_c	Pr	Nu	
					Present experiment	Numerical solution ¹
N.F.	0.25	1.07×10^6	0.702	6.18	2.67	2.65
N.F.	0.25	1.73	0.702	6.15	2.89	2.80
N.F.	0.25	2.44	0.702	6.19	2.98	2.93
N.F.	0.25	2.60	0.702	6.15	2.97	3.04
N.F.	0.50	1.68	0.700	6.34	2.00	1.98
N.F.	0.50	2.19	0.702	6.19	2.12	2.08
N.F.	0.50	2.65	0.702	6.15	2.20	2.17
N.F.	0.50	3.10	0.703	6.05	2.30	2.24
F.P.	0.25	1.02	1.018	6.15	2.35	2.27
F.P.	0.25	1.16	1.018	6.18	2.38	2.32
F.P.	0.50	1.06	1.018	6.16	1.91	1.75
F.P.	0.50	1.81	1.018	6.16	2.29	2.10
F.P.	0.50	1.88	1.020	6.11	2.32	2.12
F.P.	0.50	2.66	1.018	6.21	2.60	2.40

^a $Da = 1.048 \times 10^{-4}$ for Nickel Foametal as the porous material, $Da = 3.672 \times 10^{-4}$ for foam plastic as the porous material.

^bN.F. refers to Nickel Foametal and F.P. to foam plastic.

Table 6 Comparison of Nu for $S=1^a$

Porous material ^b	Ra_0	R_c	Pr	Nu^c	
				Present experiment	Tong and Subramanian ⁶
N.F.	126.2	0.700	6.30	1.93	1.96
N.F.	181.7	0.702	6.11	2.32	2.33
N.F.	224.0	0.703	6.07	2.60	2.57
N.F.	351.2	0.702	6.18	3.33	3.18
F.P.	380.6	1.018	6.18	3.41	3.42
F.P.	623.0	1.018	6.18	4.14	4.35
F.P.	889.3	1.018	6.22	4.78	5.16
F.P.	932.6	1.018	6.11	4.83	5.28
F.P.	1199.0	1.018	6.21	5.54	5.96

^a $Da = 1.048 \times 10^{-4}$ for Nickel Foametal as the porous material, $Da = 3.672 \times 10^{-4}$ for foam plastic as the porous material.

^bN.F. refers to Nickel Foametal and F.P. to foam plastic.

^cHere, Nu is defined as the ratio of the actual heat transfer to the heat transfer by conduction through the porous material saturated with the fluid, to be consistent with the definition in Ref. 6. Mathematically, it differs from the Nu defined by Eq. (3) by a factor of $1/R_c$.

A correlation for Nu in terms of the relevant governing parameters has been obtained for Nickel Foametal and foam plastic. The form of the correlation is

$$Nu = \frac{1}{C} + \{a_0 Ra_0^{a_1} [1 - (1-S)^{a_2}] + b_0 Ra^{b_1} (1-S)^{b_2}\} \quad (4)$$

where $C = 1.0 + S(R_c - 1)$.

The constants a_0 , a_1 , a_2 , b_0 , b_1 , and b_2 were evaluated separately for Nickel Foametal and foam plastic using software package NLIN to fit the appropriate data in Tables 1 and 2, respectively. The constants are given in Table 3. The form of the above correlation has been arrived at by assuming that the total heat-transfer rate across the enclosure is the sum of the convective and conductive components. It can easily be verified that the conductive component of Nu is proportional to $1/C$. The two terms in the square bracket on the right-hand side of Eq. (4) represent the convective components in the porous and the fluid region, respectively.

A comparison between Nu obtained from Eq. (4) and experimental Nu has been made in Figs. 6 and 8 for Nickel Foametal and foam plastic, respectively. The correlation has been depicted by solid curves. The correlation agrees with 71% of the experimental results to within 5% and with 15% of the experimental results to within 7%. The remaining results matched to within 13.4%.

To assure that the present measurements are reliable, some comparisons have been made with results from other sources. Table 4 shows such a comparison for $S=0$. This comparison shows that the largest difference from the experimental correlation presented by Seki et al.⁵ is 8.4%. For most of the results shown, the agreement is within 6%.

In Table 5, the measurements for $S=0.25$ and 0.50 have been compared with the finite-difference numerical solution developed by Tong and Subramanian.¹ It can be seen that the agreement between experiment and numerical calculation is within 9%. This difference can be accounted for in part by uncertainties in the experimental measurements of Nu and uncertainties in the data used as input in the numerical solution. The latter are a result of the experimental uncertainties in k_{eff} and κ , whose values were needed in the numerical computations.

Shown in Table 6 is the comparison for $S=1$. The results of Tong and Subramanian⁶ were obtained from a boundary-layer analysis using the Brinkman extended Darcy model. The largest difference from the measured results is 4.5%.

The fact that there are good agreements with results from other sources that include experimental, analytical, and numerical analyses should lend high confidence in the present measured Nu . In addition, the flow pattern in the fluid region for run 11 in Table 1 was photographed and is compared with the predicted streamlines in Fig. 10. The fluid was seeded with natural pearl essence to reflect light shone through a narrow slit placed at the top of the enclosure. The slit was parallel to, and midway between, the vertical end walls. The comparison shows good qualitative agreement between the experiment and the predicted results.

Conclusions

In a numerical study about heat transfer across vertical enclosures insulated with a porous insulation, Tong and

Subramanian¹ found that when R_c was <1 or ≈ 1 , heat transfer could be minimized by having only part of the enclosure filled vertically with the porous insulation. It was the objective of this study to verify experimentally the finding of Tong and Subramanian.¹

An apparatus was fabricated to simulate steady-state two-dimensional heat transfer through a vertical rectangular enclosure with an aspect ratio of 10. The thickness of the porous region was controlled in such a way that S ranged from 0 to 1. To have R_c less than 1, distilled water and Nickel Foametal saturated in distilled water were chosen as the test fluid and porous medium, respectively. To have $R_c \approx 1$, distilled water and foam plastic saturated with distilled water were chosen as the test fluid and the porous medium, respectively. For the tests conducted, R_c varied between 0.697 and 0.703 for Nickel Foametal and between 1.015 and 1.020 for foam plastic.

The heat-transfer results were presented in terms of Nu . The results showed that Nu went through a minimum when S was increased from 0 to 1. Comparisons of the present results with those in the literature yielded agreements that were better than \pm several percent. This is a strong indication that the present measurements are accurate and reliable. Furthermore, there was good qualitative agreement between a photographically recorded flow pattern and the predicted flowfield.

A correlation has been developed expressing Nu in terms of the relevant governing parameters. The present study confirms the aforementioned finding by Tong and Subramanian.¹ The finding should be useful to engineers for optimizing the performance of insulation systems, resulting in large savings in capital, as well as operating costs.

Acknowledgments

Part of this work was completed while the authors were at the University of Kentucky. The authors are grateful for the support of this work by the National Science Foundation under Grant MEA 83-08331.

References

- ¹Tong, T. W. and Subramanian, E., "Natural Convection in a Rectangular Enclosure Partially Filled With a Porous Medium," *International Journal of Heat and Fluid Flow*, Vol. 7, March 1986, pp. 3-10.
- ²Scheidegger, A. E., *The Physics of Flow through Porous Media*, 3rd ed., University of Toronto Press, Toronto, Ontario, Canada, 1974.
- ³Faruque, M. A., "An Experimental Study of Natural Convection Heat Transfer in an Enclosure Partially Filled With a Porous Medium," M.S. Thesis, University of Kentucky, Lexington, 1985.
- ⁴Sathe, S. B., "An Experimental Investigation of Natural Convective Heat Transfer in an Enclosure Partially Filled With a Porous Medium," M.S. Thesis, University of Kentucky, Lexington, 1985.
- ⁵Seki, N., Fukusako, S., and Inaba, H., "Visual Observations of Natural Convection Flow in a Narrow Vertical Cavity," *Journal of Fluid Mechanics*, Vol. 84, Nov. 1978, pp. 694-704.
- ⁶Tong, T. W. and Subramanian, E., "A Boundary-Layer Analysis for Natural Convection in Vertical Porous Enclosures—Use of the Brinkman Extended Darcy Model," *International Journal of Heat and Mass Transfer*, Vol. 28, March 1985, pp. 563-571.